.1

Part I

Introduction: General Observations of the ISM

Contents

.2

1 The Galactic environment of the Sun

1.1 The very local ISM

The very local ISM

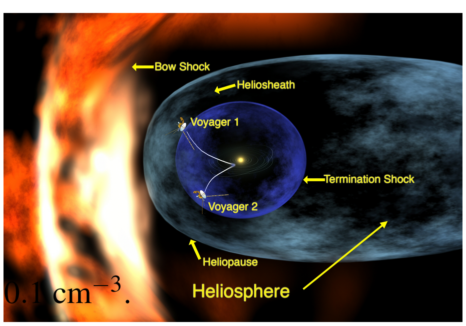

The Solar wind blows out a cavity inside the local ionised cloud (LIC). The heliosphere is about 100 AU in diameter, with $N_e \sim 1 \times (1/(r/\mathrm{AU})^2)$ cm^{-3}, and $T_e \sim 10^4$ K. Optical absorption lines in the LIC have $W_\lambda \sim$ 200 mÅ, b ~1 km s^{-1}, and correspond to a singly ionised gas with $T_e \sim 7000$ K, $N_e \sim$ 0.1 cm^{-3}.

The LIC is embedded in the Local Bubble, $N_e \sim 5\ 10^{-3}$ cm^{-3}, $T_e \sim 10^6$ K.

Vallerga et al. (1993) show that the local ISM, the bulk of clouds within the Local Bubble, is at rest in the LSR ± 11 km s^{-1} as traced by CaII, and ± 3.6 km s^{-1} as traced by Na I. The solar motion relative to the LSR is about 20 km s^{-1} in the direction of Scorpius. .3

Crude measures of the very local ISM density

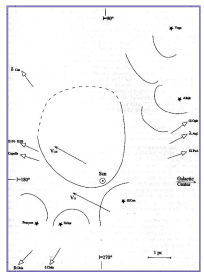

`Ferlet 1999, A&ARv, 9, 153` .4

1.2 The Local Bubble

The Local Bubble.

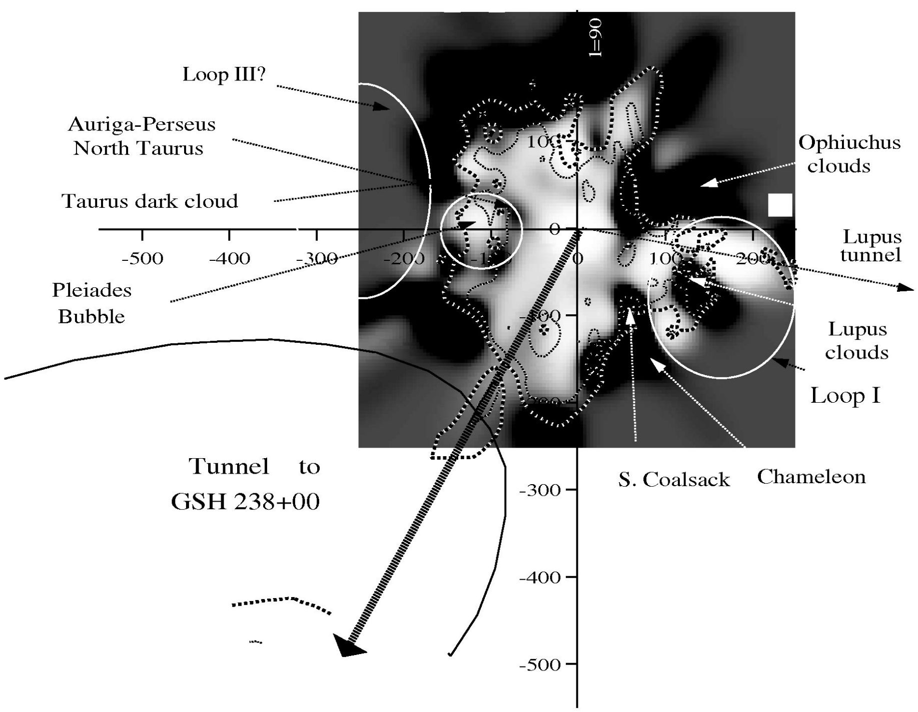

Na D lines maps. Contours at $W_\lambda = 20$ mÅ and 50 mÅ . Lallement et al. (2003, A&A 411, 447). .5

The Local Chimney

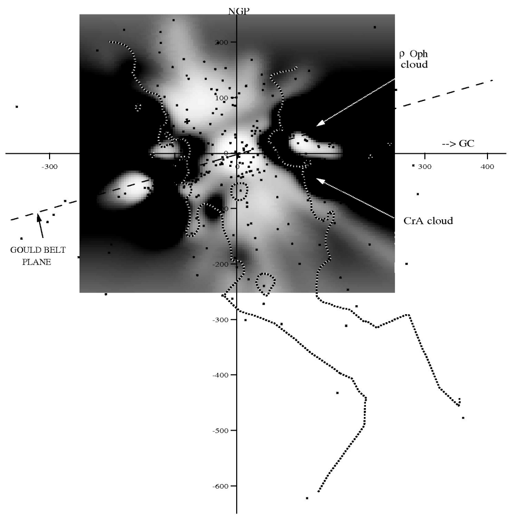

- The Local Bubble appears to be squeezed into a Local Chimney by SNR shells. The Local Chimney is very narrow: about 20 deg towards each Galactic pole, corresponding to directions of minimal diffuse Hα and far-IR.

.6

Extragalactic windows

Lallement et al. (2003) explain that “no distinct and continuous neutral boundary to the ends of the Local Chimney has been found in either galactic hemisphere for distances <400 pc”. Crawford et al. (2002) favor a picture of the inner galactic halo in which a population of infalling IVCs lie along the Local Chimney.

$\rightarrow$ The main absorbers in the local ISM towards extragalactic objects are probably the boundaries of the Local Chimney. .7

Further 3D maps of the local ISM: face-on

New density fields from Welsh, Lallement et al., 2010, A&A, 510, A54

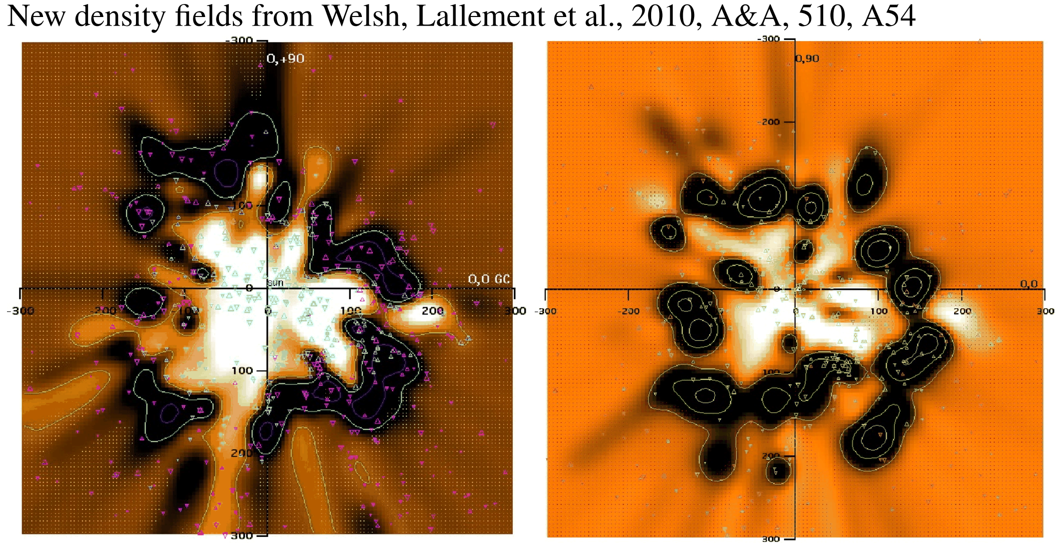

Na I   Ca II .8

Further 3D maps of the local ISM: side view

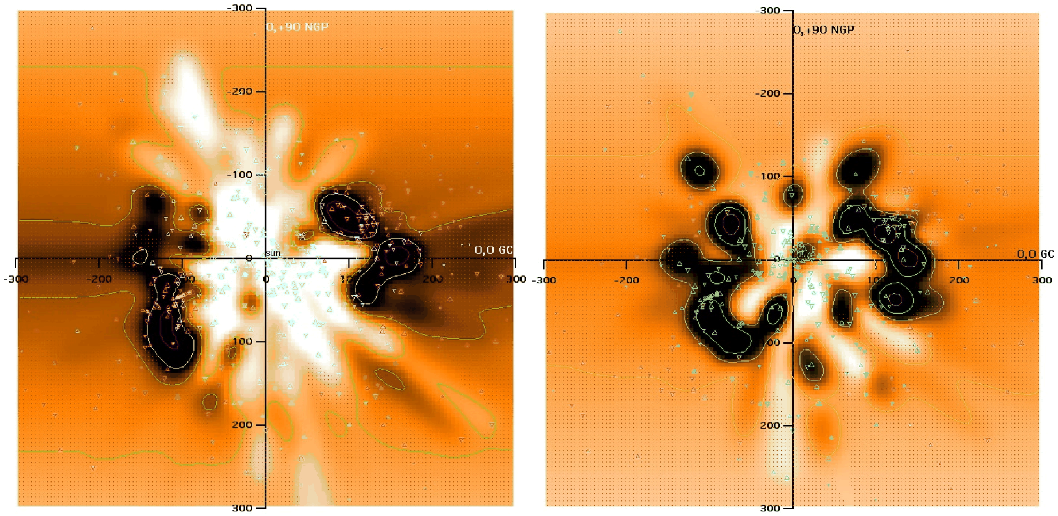

Na I   Ca II

.9

2 Morphology of interstellar clouds

2.1 Old model for clouds in thermal equilibrium

Morphology of interstellar clouds

Interstellar absorption lines (e.g.: $CH^{+}\lambda 4232$Å, $CH\lambda 4300$Å, $CN\lambda 3875$Å, etc..., ref: Dunham 1937, PASP, 49, 26; Douglas & Herzberg 1941, ApJ, 94, 381; Adams 1949, ApJ, 109, 354)

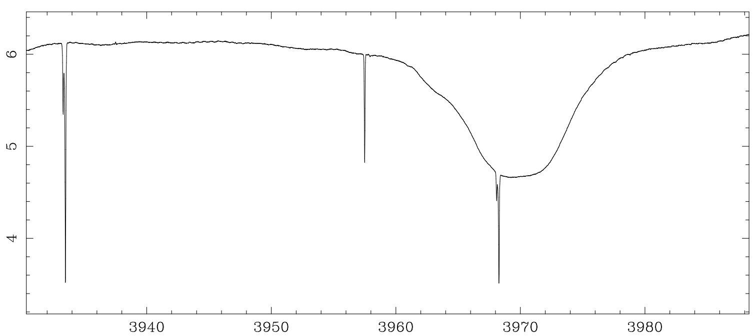

ζOph VLT+UVES spectrum around ∼3960Å

.10

Old model

ζOph VLT+UVES spectrum around ∼3960Å- zoom.

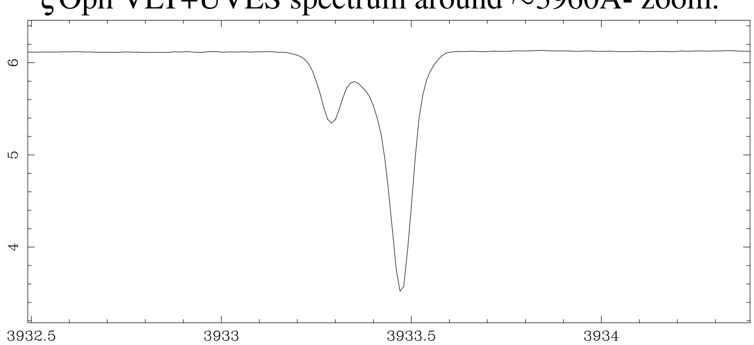

$\rightarrow$ model of discrete clouds confined by pressure equilibrium with the the intercloud medium, $T \sim 10^6$K (e.g. Spitzer, 1956, ApJ, 124, 20), confirmed through the observation of O VIλ1031 absorption towards nearby stars (*Copernicus*$\sim$1973, *FUSE* $\sim$2002). .11

2.2 Realistic descriptions

Problems with the discrete cloud model

(Elmegreen & Falgarone, 1996, ApJ, 471, 816)

- Supersonic motions imply that the dynamics of the clouds are dominated by shocks, not thermal pressure.
- Improving the angular resolution of interstellar cloud maps invariably result in the discovery of substructure.
- Linear size, mass, and velocity dispersion are related by power laws, which can be characterised through scaling laws: $N(L) \propto M(L) \propto L^D$. Power laws are typical of self-similar structures. A function $y = f(x)$ whose properties only change by a factor b when applying a scaling factor $a \times x$ must fulfill $f(ax) = bf(x)$. Scaling k times, $x = a^k x_\circ$, and $y = b^k y_\circ$, from which $y = x^c$, with $c = \ln(b)/\ln(a)$. If y is the number of structures or the mass, and if x is size, then c is the fractal dimension of the selfsimilar structure.

.12

Morphology of the ISM: scaling laws

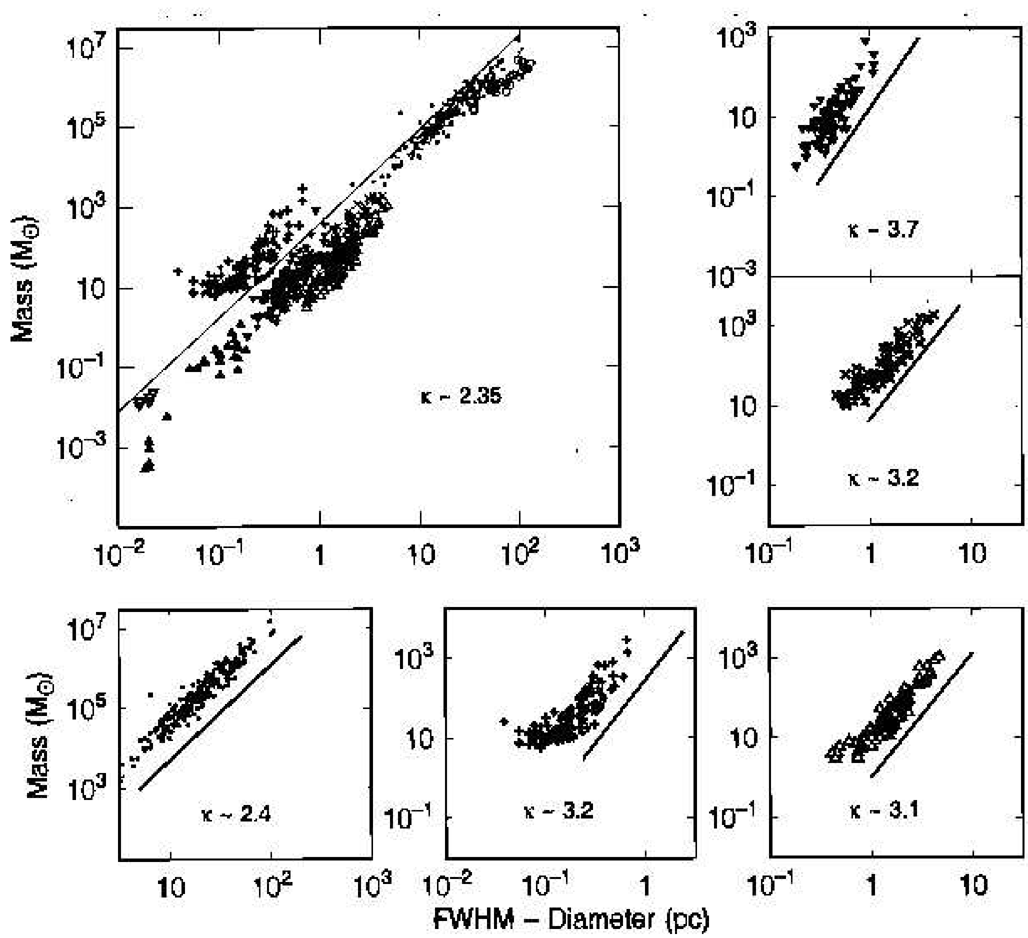

.13

Morphology of the ISM: Armonic analysis

The structure of the ISM can also be described by an armonic analysis, with the power spectrum of the specific intensity maps: $P(k) \propto k^{\alpha}$, in which $P(k)$ is the modulus of $F(k) = \int dxdyI(x,y)\exp(2i\pi\vec{k}.\vec{x})$, with an angle average for isotropic distributions. The power spectrum allows the inference of basic properties of the emission maps, such as characteristic angular sizes, relative importance of angular scales, etc....

For scales larger than >10 deg, it is necessary to take into account the curvature of the celestial sphere:

$$I(\hat{r},\nu) = \sum_{l}\sum_{m} Y_{lm}(\hat{r})a_{lm}(\nu),$$

and the power spectrum is $C_l \equiv 1/(2l+1)\sum_{m=-l}^{m=+l}\langle\|a_{lm}(\nu)\|^2\rangle$, in the definition by Tegmark & Efstathiou, 1996, MNRAS, 281, 1297. In a flat aproximation to the celestial sphere, $k = (l+1/2)/2\pi$, and $k^2P(k) = l(l+1)C_l/(2\pi)^2$, with k in rad^{-1}. .14

Example power spectra

- CMB.
- white noise, with $P(k) = \text{Cte}$. Example: point sources with a random distribution (i.e. Poisson). On average, $\langle a_{lm} \rangle = \int d\Omega \, Y^{\star}_{lm}(\Omega) \langle I(\hat{r}) \rangle$, with $\langle I(\hat{r}) \rangle = \frac{N}{4\pi}\phi$, where ϕ is the average flux density of N sources in the sky. $\langle n \rangle = N/4\pi$ follows a Poisson distribution: $\langle n^2 \rangle - \langle n \rangle^2 = \langle n \rangle$. $\langle \|a_{lm}\|^2 \rangle = \int d\Omega d\Omega' \, Y^{\star}_{lm}(\Omega) Y_{lm}(\Omega') \, \langle I(\Omega) I(\Omega') \rangle \rangle$, and as $\langle I(\Omega) I(\Omega') \rangle = \delta(\Omega - \Omega') \phi^2 \langle n \rangle \Rightarrow C_l = \phi^2 \langle n \rangle$.
- power spectrum of the *IRAS* syrvey. Ref: Gautier et al. (1992, AJ, 102, 1313), Miville-Deschêches et al. (2007, A&A, 469, 595): $P(k) \propto k^{-2.9}$.
- Recent analysis by Oliveira-Costa et al. (2002, ApJ, 567, 363).

.15

ISM power spectra

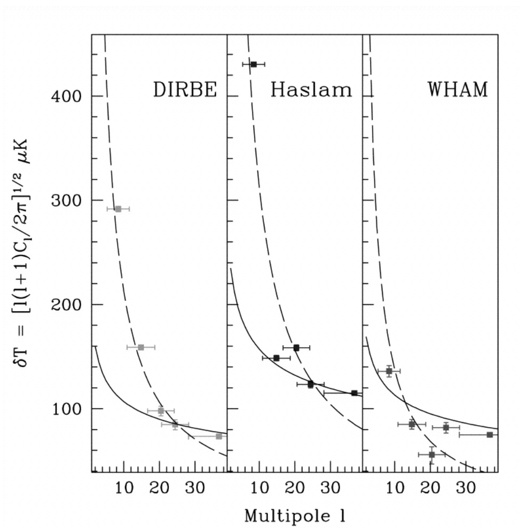

.16

Morphology of the ISM: armonic analysis

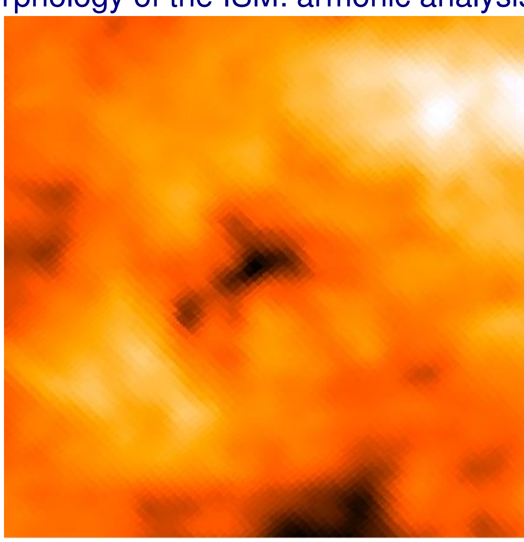

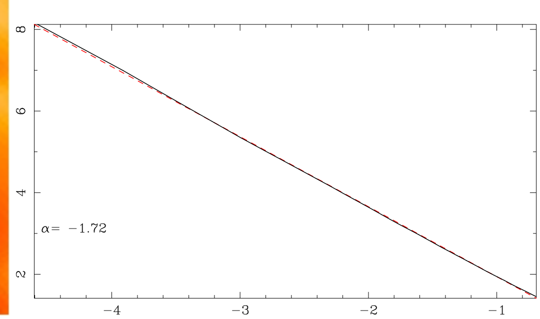

.17

Morphology of the ISM: relationship between scaling laws and the power spectrum

A self similar structure with a self-similar exponent H has a 1-D power spectrum $P(k) = \mathrm{Cte}\ k^{-1-2H}$ (e.g. “Fractals, a User’s Guide for the Natural Sciences”, Hastin & Sugihara, 1993, Oxford Science Publications).

A recipe for simulating fractals is therefore to generate a power-spectrum whose amplitude has a variance of k^{-1-2H}, and with random phases. Passing to the celestial plane and taking real parts, one gets a self-similar structure with fractal dimension $2H$, and with random phases. Switching to the image plane and taking real parts one obtains a self-similar structure with fractal dimension $2H$, and with random phases. The requisite $P(\hat{k}) = P^{\star}(-\hat{k})$ generates a real map.

.18

Morphology of the ISM: examples

Fractal analysis of an H I 21 cm in the LMC (Elmegreen, Kim, Staveley-Smith ,2001,ApJ,548,749)x.

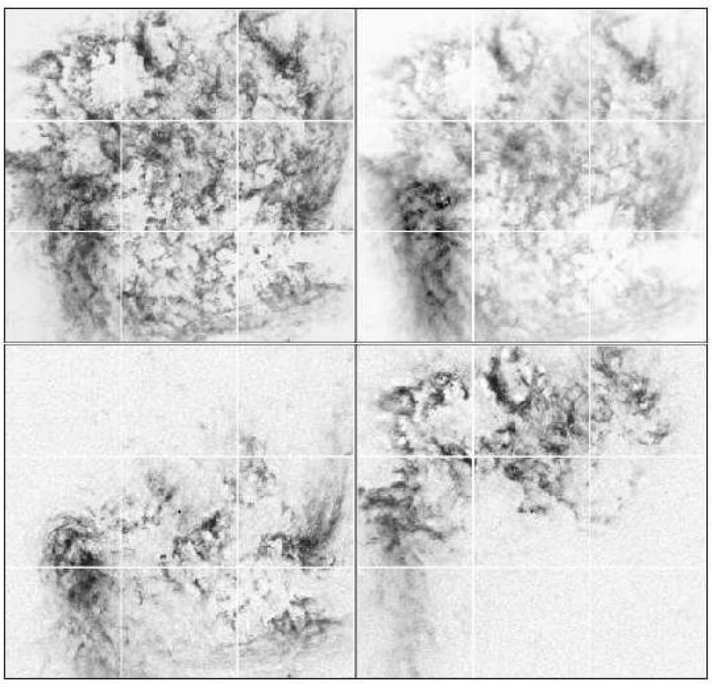

.19

Morphology of the ISM: examples

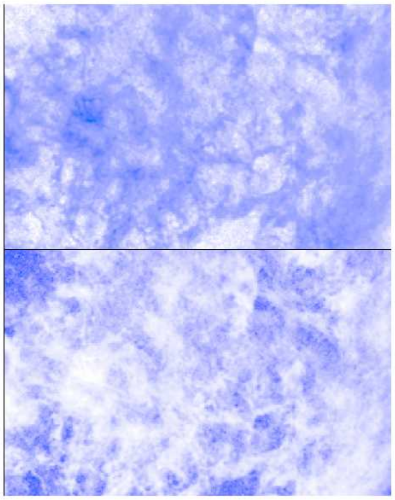

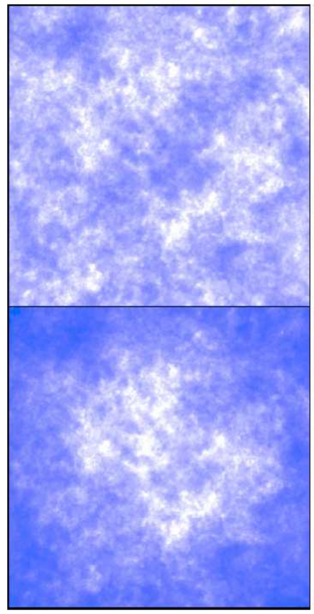

.20

3 Phases of the ISM

Phases of the ISM

Molecular components (H_2), atomic (H I, photo-dissociation regions, or PDRs), ionised (H II regions, with T 10^4 K), and hot plasma, with T 10^6 K.

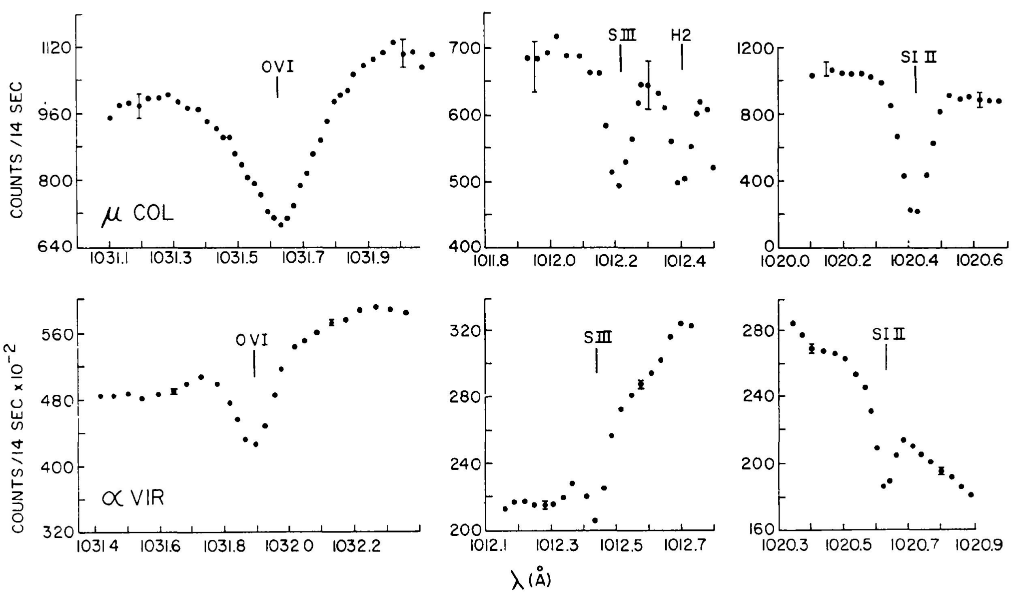

.21

Phases of the interstellar medium: dust in the H I region

Depletion pattern in the neutral phase of the ISM towards ζOph $\rightarrow$ dust at 18 K. .22

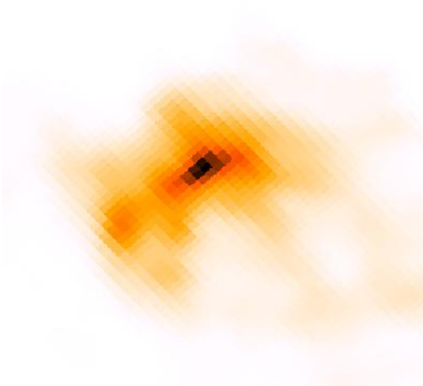

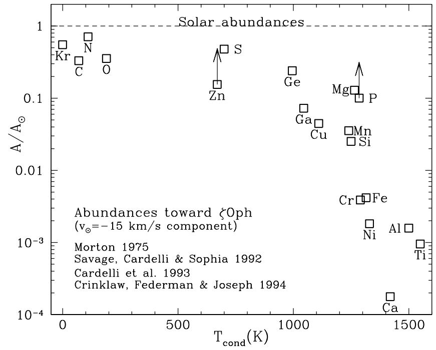

http://skyview.gsfc.nasa.gov

4 Mixing in the ISM

Mixing in the ISM

The isotopic ratio $^{12}C/^{13}C$ is a good tracer of the stellar processing of the ISM.

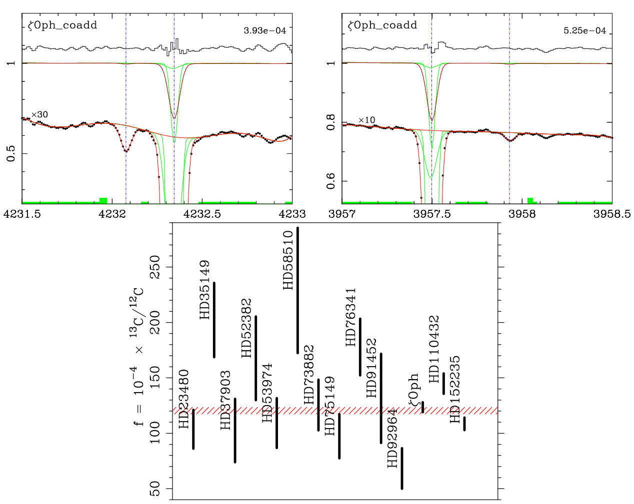

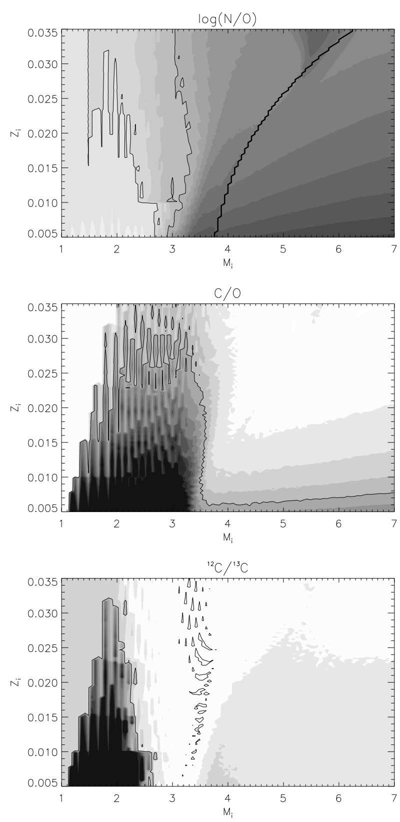

.23

5 Emission mechanisms in the ISM

Emission mechanisms in the ISM - synchrotron

http://lambda.gsfc.nasa.gov/product/map/

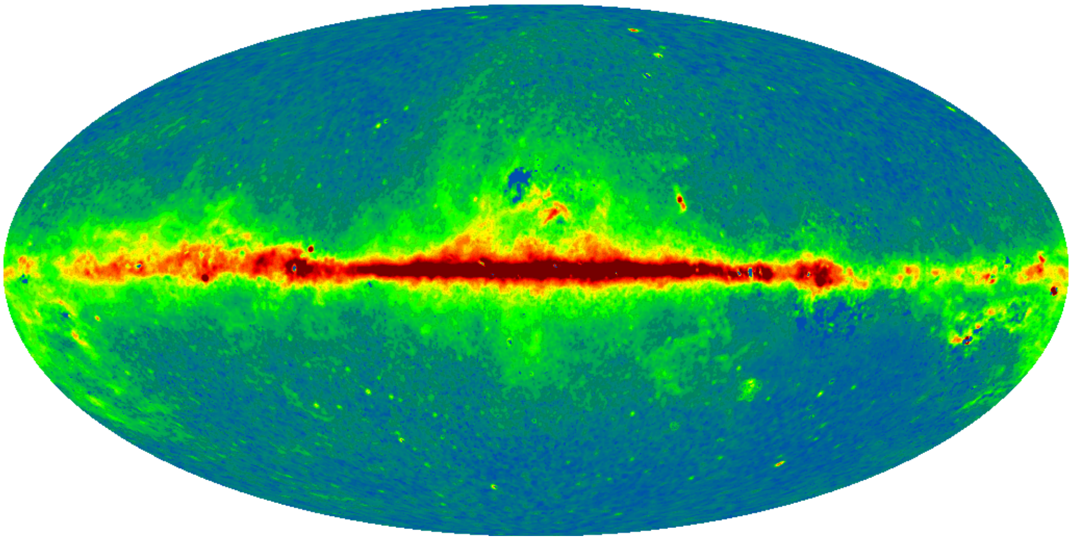

.24

Emission mechanisms - free-free

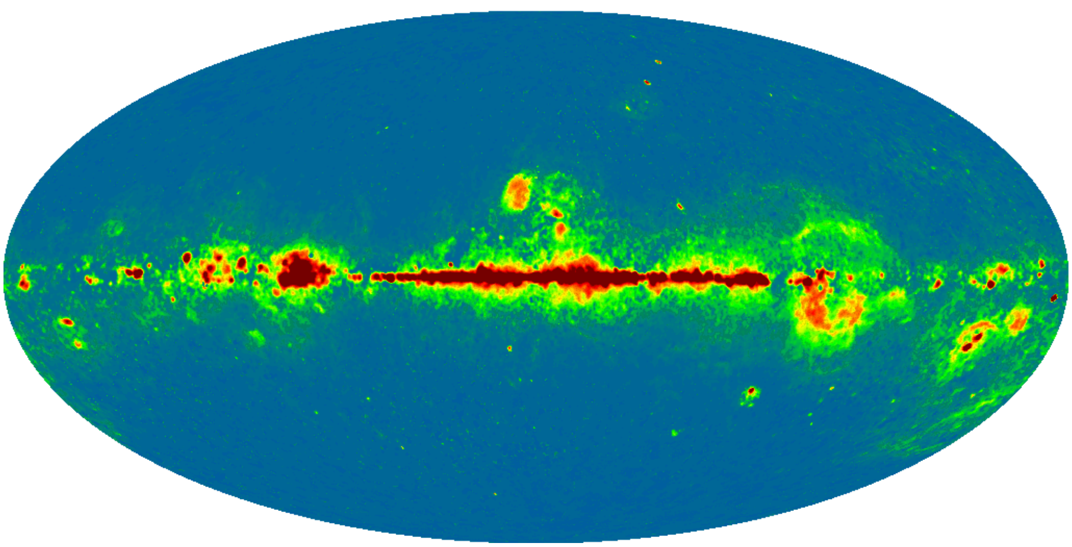

.25

Emission mechanisms - standard dust

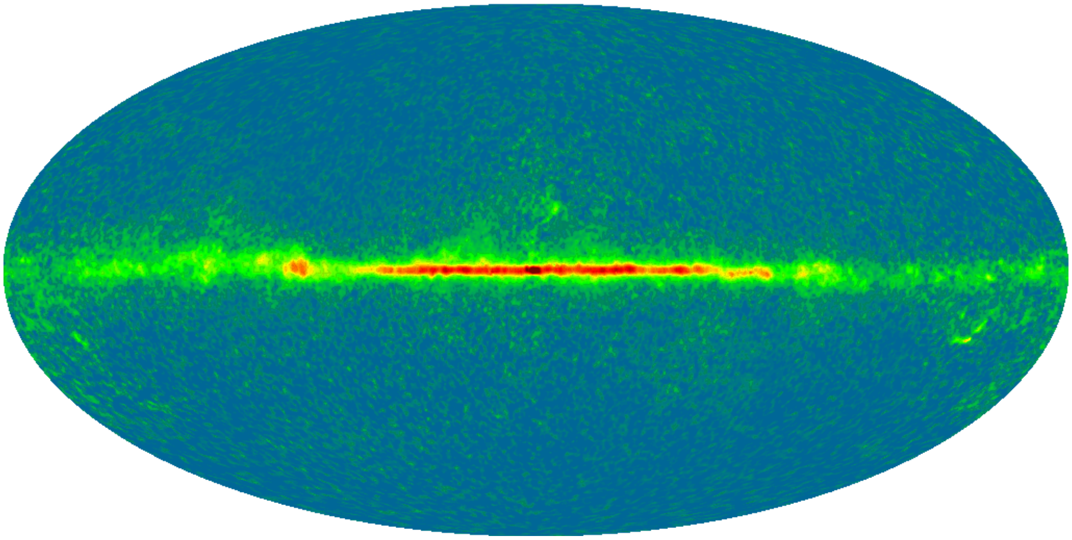

.26

6 Conspicuous features

Conspicuous features

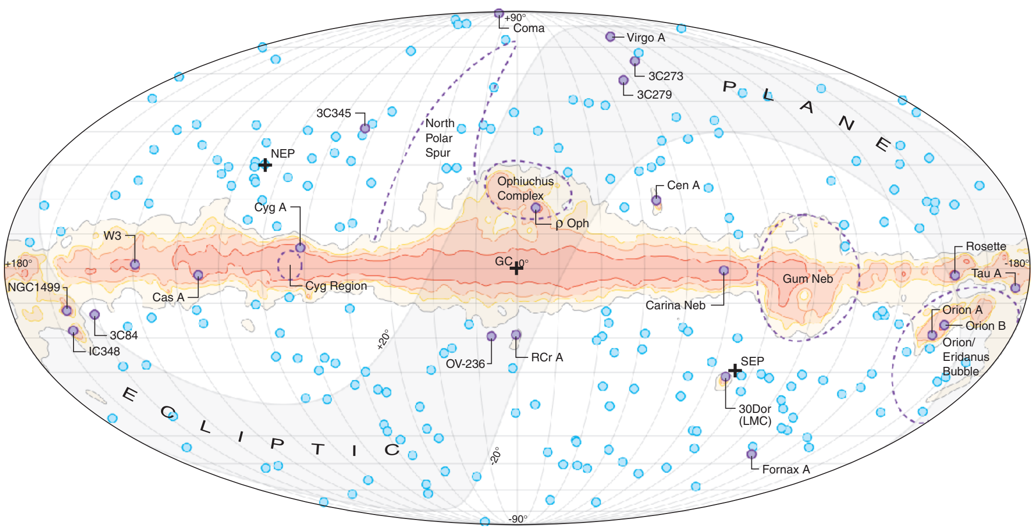

.27

Conspicuous features - Planck

http://www.esa.int/SPECIALS/Planck/index.html

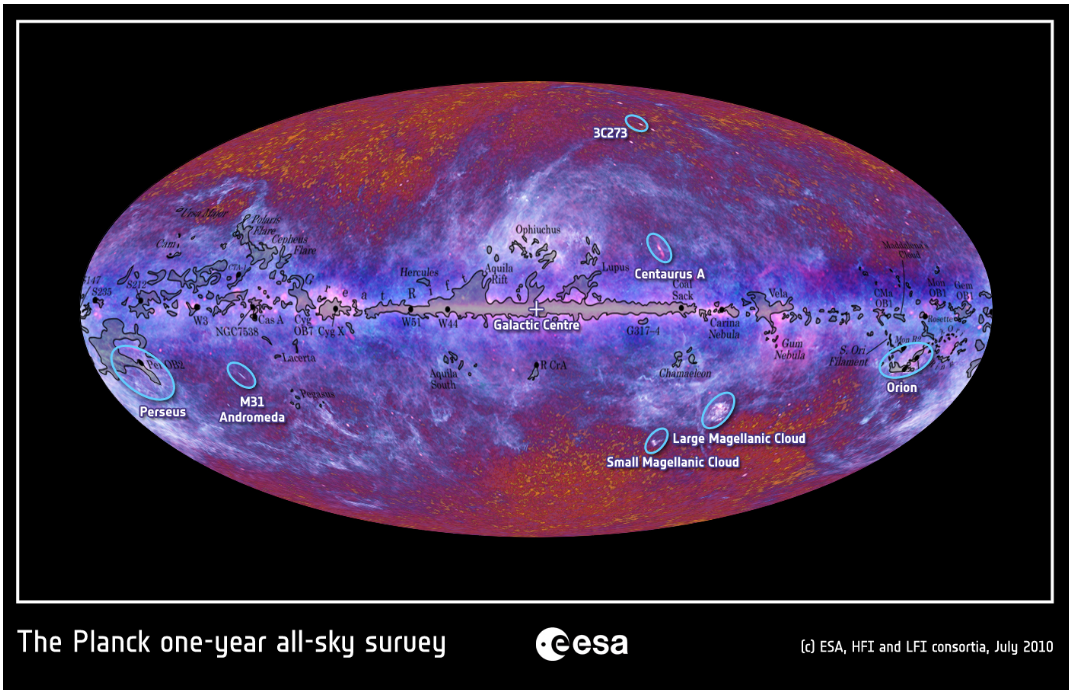

.28

Example star forming region: Aquila Rift - Planck

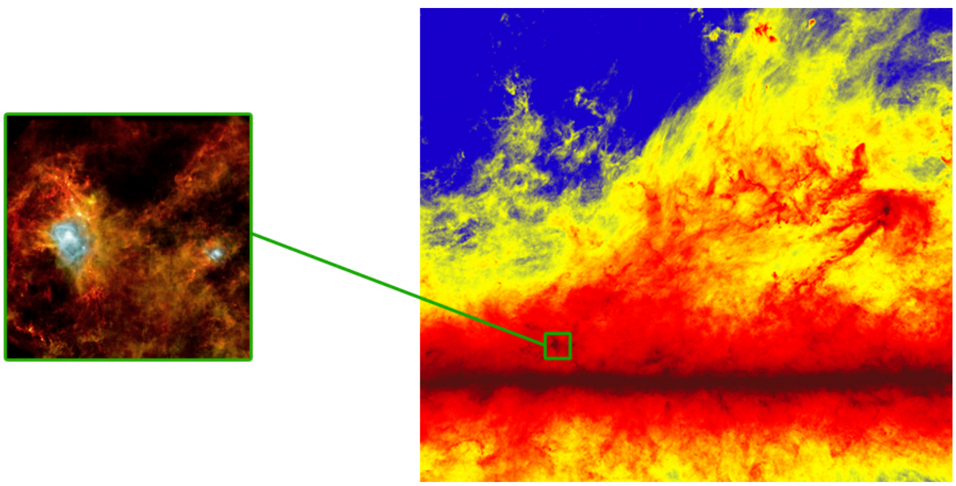

Left: Herschel, Right: Planck

.29